AGU100 ADVANCING EARTH AND SPACE SCIENCE

Water Resources Research

RESEARCH ARTICLE
10.1029/2019WR025166

Key Points:
- Traditional interpretations of the response of unconfined aquifers to solid Earth tides ignore capillary effects
- Here we use a numerical procedure to study the capillary effects on the response of unconfined aquifers to Earth tides
- We show that the capillary effects are important in influencing the response of unconfined aquifer to Earth tides and need to be considered

Supporting Information:
- Supporting Information S1

Correspondence to:
C.-Y. Wang,
chiyuen@berkeley.edu

Citation:
Wang, C.-Y., Zhu, A.-Y., Liao, X., Manga, M., & Wang, L.-P. (2019). Capillary effects on groundwater response to Earth tides. *Water Resources Research*, *55*, 6886–6895. https://doi.org/10.1029/2019WR025166

Received 15 MAR 2019
Accepted 14 JUL 2019
Accepted article online 24 JUL 2019
Published online 19 AUG 2019

Capillary Effects on Groundwater Response to Earth Tides

Chi-Yuen Wang[1], Ai-Yu Zhu[1,2], Xin Liao[3], Michael Manga[1], and Lee-Ping Wang[4]

[1]Department of Earth and Planetary Science, University of California, Berkeley, CA, USA, [2]Institute of Geophysics, China Earthquake Administration, Beijing, China, [3]Institute of Disaster Prevention, Beijing, China, [4]Department of Chemistry, University of California, Davis, CA, USA

Abstract The response of unconfined aquifers to Earth's solid tides (Earth tides) has been used to study a number of hydrogeological, environmental, and ecological processes. The traditional interpretation of such responses has been based on a model that assumes free flow of groundwater to the water table, even though capillary effects have long been recognized to influence the response of coastal aquifers to ocean tides. Here we study the capillary effect on the response of unconfined aquifers to Earth tides, using a numerical procedure that couples groundwater flow and poroelastic strain in both the saturated and the unsaturated zones. We show that when the water table rises to the surface and the capillary zone disappears, the predicted tidal response is identical to that predicted by the traditional model. But when the capillary zone is present when the water table falls below the surface, the predicted amplitude ratio and phase shift depart notably from those predicted by the traditional model. We apply the model to a field case where large seasonal changes of tidal response have been documented. We show that the large seasonal changes in the tidal response may be due to the change of the water table from a capillary-affected state to a capillary-free state when the water table rises annually to the ground surface. Thus, the omission of the capillary effects in the interpretation of the response of unconfined aquifers to Earth tides may lead to incorrect inference of subsurface processes and properties.

1. Introduction

The response of coastal aquifers to ocean tides has been known for millennia (Pliny the Elder, circa AD 77–79). In contrast, the response of aquifers to Earth's solid tides (Earth tides) was not documented until the twentieth century (e.g., Bredehoeft, 1967), probably due to its small amplitude. On the other hand, unlike ocean tides that are limited to coastal areas, Earth tides affect the entire globe; thus, the response of aquifers to Earth tides has been measured and used to study hydrogeological, environmental, and ecological processes across the continents (e.g., Allègre et al., 2016; Barbour et al., 2019; Bredehoeft, 1967; Elkhoury et al., 2006; Liao & Wang, 2018; Roeloffs, 1996; Rojstaczer & Riley, 1990; Wang et al., 2018; Xue et al., 2016). Because of their small magnitude relative to ocean tides, Earth tides are usually studied at sites away from the coast where the effects of ocean tides may either be neglected or be removed by analysis. In addition, the interpretation of the response of aquifers to Earth tides requires the coupling of poroelastic deformation of the aquifer to groundwater flow; thus, its mathematical formulation is significantly different from that used in the study of the response to ocean tides.

Interpretation of the response of unconfined aquifers to Earth tides in the past 50 years has been based on a model that assumes free flow of groundwater to the water table (e.g., Allègre et al., 2016; Barbour et al., 2019; Bredehoeft, 1967; Bower & Heaton, 1978; Doan et al., 2006; Liao & Wang, 2018; Rojstaczer & Riley, 1990; Roeloffs, 1996; Wang, 2000; Xue et al., 2016). This assumption is convenient, but, if the water table is below the ground surface, a zone of partially saturated material occurs above the water table and the capillary force between pore water and the surfaces of solid grains may affect groundwater flow. It is well known that the capillary force acts to pull groundwater upward against gravity, forming a zone of negative pressure and variable saturation. We refer to this zone of variable saturation and negative pressure as the "capillary zone" (Barry et al., 1996) and reserve the term "capillary fringe" for the saturated portion of this zone at its base (e.g., Bear, 1972; Gillham, 1984; Meinzer, 1923), even though the latter is sometimes used for the entire zone of variable saturation (e.g., Nielsen & Perrochet, 2000). The importance of the capillary zone on the response of coastal aquifers to ocean tides and waves has long been recognized (e.g., Barry et al., 1996; Kong et al., 2013; Li et al., 1997; Nielsen & Perrochet, 2000; Parlange & Brutsaert, 1987; Shoushtari et al., 2015;

Turner & Nielsen, 1997) but has largely been ignored in the studies of aquifers' response to Earth tides, except in some efforts to account for air diffusion in the unsaturated zone under barometric loading (e.g., Roeloffs, 1996; Rojstaczer, 1988; Rojstaczer & Riley, 1990).

Here we use a numerical procedure that incorporates coupled groundwater flow and the poroelastic strain produced by Earth tides, both in the saturated and in the unsaturated zones, to explore the effect of the capillary force on the tidal response of unconfined aquifers. We show that the capillary force may significantly influence the response of groundwater to Earth tides in ways unexpected from the traditional model, and we demonstrate the importance of this effect with a field example and numerical simulation and show that the capillary effect can explain some previously puzzling observations.

2. Model Development

The Boussinesq equation was modified to account for capillarity effects on water table fluctuations in coastal aquifers responding to the boundary loading of ocean tides (e.g., Barry et al., 1996; Kong et al., 2013; Parlange & Brutsaert, 1987). In contrast, the investigation of the capillary effect on the response of aquifers to Earth tides requires the coupling of the time-dependent, poroelastic deformation of the solid matrix and the induced pore pressure and flow. Biot (1941) formulated the equations for coupled flow and deformation in saturated poroelastic media. Here we extend this formulation to include both the saturated and the unsaturated poroelastic media. In the absence of a fluid source, the equation of continuity for pore water of constant density is

$$\frac{\partial \theta}{\partial t} = -\nabla \cdot \boldsymbol{q} \tag{1}$$

where θ is the water content in a unit volume of a variably saturated media and $\boldsymbol{q}$ the specific discharge vector. For unsaturated flow in the vertical direction we have (Richards, 1931)

$$q_z = -K(\theta)\left(\frac{\partial h_p}{\partial z} + 1\right) \tag{2}$$

where $K(\theta) = k_r K_s$ is the unsaturated vertical hydraulic conductivity and is a function of the water content, k_r is the relative conductivity, K_s is the saturated vertical hydraulic conductivity, h_p is the pressure head of the capillary water that is equal to $p/\rho g$, ρ is the density of groundwater, g is the gravitational acceleration, and z is the elevation above a vertical reference.

In the absence of fluid sources, the water content θ in an isotropic, partially saturated poroelastic medium is a function of the volumetric stress σ and pore pressure p; thus, the change of water content may be expressed as (Wang, 2000, p.35)

$$\mathrm{d}\theta = S_\sigma(\theta)[B(\theta)\mathrm{d}\sigma + \mathrm{d}p], \tag{3}$$

where $S_\sigma(\theta) \equiv (\partial\theta/\partial p)_\sigma$ is the "unconstrained" storage for the unsaturated zone, and $B(\theta)$ is Skempton's coefficient for the unsaturated zone. The differences among all the storages defined under different boundary conditions are small; thus, we may be justified to generalize the unconstrained storage here to one for conventional aquifer conditions (Green & Wang, 1990). Following Bear (1972), we express the storage as $(C(\theta)+S_eS_s)/\rho g$ to include both the saturated and unsaturated media, where $C(\theta) = \partial\theta/\partial h_p$ is the specific moisture capacity, S_s is the specific storage for saturated media, and S_e is the effective saturation defined as

$$S_e = (\theta - \theta_r)/(\theta_s - \theta_r), \tag{4}$$

where θ_r and θ_s are, respectively, the residual and the saturated water content, and we rewrite (3) as

$$\mathrm{d}\theta = (C(\theta) + S_eS_s)(B(\theta)\mathrm{d}\sigma + \mathrm{d}p)/\rho g. \tag{5}$$

Combining equations (1), (2), and (4), we obtain

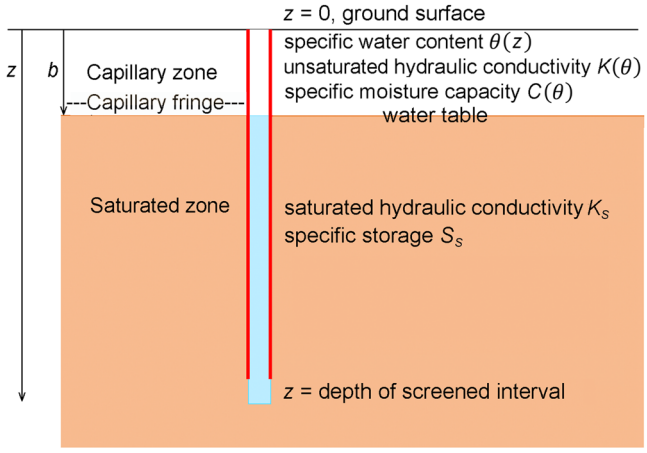

Figure 1. Schematic illustration of a well in an unconfined aquifer defining key variables.

$$\frac{\partial}{\partial z}\left[K(\theta)\left(\frac{\partial h_p}{\partial z}+1\right)\right]=(C(\theta)+S_eS_s)\left(\frac{B(\theta)}{\rho g}\frac{\partial \sigma}{\partial t}+\frac{\partial h_p}{\partial t}\right). \quad (6)$$

Given the very long wavelengths of the diurnal and semidiurnal tides, groundwater in the aquifer may be considered undrained during tidal deformation; thus, $\sigma = K_u\varepsilon$, where K_u is the undrained bulk modulus of the aquifer and ε is the poroelastic volumetric strain produced by Earth tides; thus, equation (6) may also be expressed as

$$\frac{\partial}{\partial z}\left[K(\theta)\left(\frac{\partial h_p}{\partial z}+1\right)\right]=(C(\theta)+S_eS_s)\left(\frac{B(\theta)K_u}{\rho g}\frac{\partial \varepsilon}{\partial t}+\frac{\partial h_p}{\partial t}\right). \quad (7)$$

Under saturated conditions, $C(\theta) = 0$, $S_e = 1$, $B(\theta) = B$, and $K(\theta) = K_s$, and the above equation reduces to the traditional equation for the tidal effect on saturated flow in unconfined aquifers (e.g., Doan et al., 2006; Roeloffs, 1996; Wang, 2000).

For our simulation we apply equation (7) to a column of uniform sediments extending from the ground surface to infinite depth (Figure 1) that includes an unsaturated zone above the initial water table at depth b below the ground surface and a saturated zone below the water table. A no-flow boundary condition is assigned at infinite depth; that is,

$$\boldsymbol{q} = 0 \text{ at } z = \infty, \quad (8)$$

and a mixed boundary condition is assigned at the ground surface; that is,

$$\boldsymbol{q} = -k_rK_sh_p/b \text{ at } z = 0. \quad (9)$$

Equation (9) is a type of boundary condition used in numerical simulation of problems where the boundary condition depends on solution such as seepage-face formation, evapotranspiration, and rainfall infiltration (Chui & Freyberg, 2009; Shoushtari et al., 2015). The advantage of using equation (9) is that it adjusts to the dynamic changes of boundary conditions without additional checks. For the present case, the water table oscillates due to seasonal and tidal forcing. When the depth of the water table is greater than the thickness of the capillary fringe, $S_e(z = 0)$ 0 and $k_r(z = 0)$ 0 (equation (11)), and (9) is a no-flow condition. On the other hand, when the water table reaches the ground surface, that is, $b =$ 0, $k_rK_s/b = K_s/b$ ∞, and (9) becomes a free-flow condition.

We allow the simulation to run long enough that transient effects from an arbitrary initial condition have decayed and a quasi steady state has been reached; the behavior of the system is then entirely controlled by the boundary conditions and the hydraulic and poroelastic properties.

A large amount of experimental measurements has been accumulated for the hydraulic properties of unsaturated sediments (e.g., Carsel & Parrish, 1988; Muñoz et al., 2003; Villar, 2007), and several empirical relations have been developed to fit the experimental data (e.g., Corey, 1957; Fredlund & Xing, 1994; Mualem, 1976; Van Genuchten, 1980). Here we adopt the van Genuchten relation between the effective saturation $S_e(\theta)$ and the capillary pressure head h (Van Genuchten, 1980)

$$S_e(\theta) = [1 + (\alpha h)^n]^{-m}, \quad (10)$$

the van Genuchten-Mualem relation for the relative conductivity $k_r(\theta)$ (Mualem, 1976)

$$k_r(\theta) = S_e^{\,l}\left[1-\left(1-S_e^{\frac{1}{m}}\right)^m\right]^2, \quad (11)$$

and the van Genuchten relation for the specific moisture capacity $C(\theta)$ (Van Genuchten, 1980)

Table 1
Poroelastic and Hydraulic Parameters Used in the Present Simulation

Parameter	Silt	Sand	References	Model in Figure 6
K_s (m/s)	10^{-6}	10^{-4}	Fetter (2001)	2×10^{-6}
S_s (m^{-1})	10^{-4}	10^{-5}	Fetter (2001)	10^{-6}
θ_s	0.46	0.43	Carsel and Parrish (1988)	0.46
θ_r	0.034	0.045	Carsel and Parrish (1988)	0.034
α (m^{-1})	1.6	14.5	Carsel and Parrish (1988)	8
n	1.37	2.68	Carsel and Parrish (1988)	1.37
l	0.5	0.5	Carsel and Parrish (1988)	0.5

Note. α, n, and l are fitting parameters in the empirical van Genuchten model.

$$C(\theta) = \frac{\alpha\, m}{1-m}(\theta_s - \theta_r) S_e^{\frac{1}{m}} \left(1 - S_e^{\frac{1}{m}}\right)^m, \tag{12}$$

where α,l, m, and n are fitting parameters in the empirical relations for fitting experimental data for unsaturated sediments.

Although the parameter B changes with θ in the unsaturated zone, the change of pore pressure occurs mostly in the saturated zone that is volumetrically much larger; thus, the change of B with θ in the unsaturated zone should have a minimal effect on the tidal response.

3. Simulation and Results

In this section we compare the tidal response of a fine-grained silt aquifer with that of a coarse-grained sand aquifer. The empirical parameters for these sediments are listed in Table 1. As a first approximation, we do not consider the hysteresis of hydraulic properties. Application of the simulation to a specific field case is discussed in the next section.

Because the hydraulic properties of unsaturated sediments depend on water content, Richards equation is nonlinear and equation (7) cannot be easily solved analytically. We thus use a finite element method, constrained by boundary conditions (8) and (9) and the experimental data in Table 1, to find the solutions. We use a commercially available software package, COMSOL, to implement the simulations. Small element size and time steps are required to ensure accuracy and numerical stability. We follow the usual approach to use the semidiurnal lunar tide (i.e., the M_2 tide) in the simulation, because this tidal component has relatively large amplitude and is relatively free of thermal and barometric disturbances.

Figure 2 shows an example of the simulated steady oscillations of the responding pressure head in a silt aquifer at a specified average water table depth of $b = 0.5$ m (Figure 1). It shows that, with decreasing screened depth z (Figure 1), the amplitude of the oscillation decreases and the phase increases. The amplitude ratio and phase shift, calculated in reference to the driving head, are plotted against the dimensionless depth z/δ to produce the curve labeled with $b = 0.5$ m in Figure 3a, where $\delta = \sqrt{2D/\omega}$, $D \equiv K_s/S_s$ and ω is the angular frequency of the M_2 tide. By setting the average water table at different depths, we obtain the set of curves in Figure 3a. For the sand aquifer, we similarly obtain a set of curves following the same procedure and plot the curves in Figure 3b.

For the sake of comparison, we also plot in Figure 3 the predicted tidal response for the traditional model of unconfined aquifers (Doan et al., 2006; Roeloffs, 1996; Wang, 2000). Both Figures 3a and 3b show that the present model predicts the same tidal response as the traditional model when the average water table is at the ground surface. But when the water table falls below the ground surface, the predicted amplitude ratio and phase shift depart significantly from those of the traditional model. For the silt aquifer (Figure 3a), the departure between the two models increases gradually with increasing water table depth until the latter reaches ~2 m below the ground surface where the amplitude ratio becomes 1 and the phase shift becomes 0. For the sand aquifer (Figure 3b), on the other hand, this transition occurs abruptly when the water table drops below the ground surface.

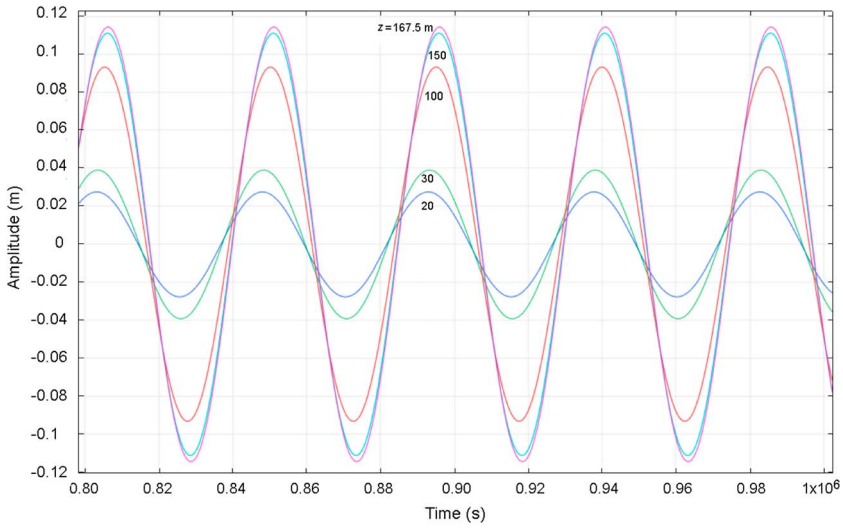

Figure 2. Simulated water level oscillations in a silt aquifer in response to the M_2 tide when the average water table depth is 0.5 m. Numbers on the curves mark the depth of the screened interval of the well.

We attribute the change in tidal response with water table depth to the truncation of the capillary zone when the water table approaches the surface, a mechanism clearly illustrated in sand column experiments (Cartwright et al., 2005). Figure 4 shows the simulated profiles of S_e, k_r, and θ in sand and silt when the water table is at 0.5 m below the ground surface. The capillary zone for the silt aquifer in this case is largely truncated by the surface, while that for the sandy aquifer is relatively unaffected, a difference directly related to the different thicknesses of the capillary zone in the two aquifers. When the water table is at the surface, the capillary zone is removed and the simulated results match the traditional model perfectly; but when the water table is below a threshold depth beneath the surface, which depends on aquifer properties, the presence of the capillary zone substantially alters the tidal response of the aquifer; the response and the tidal forcing become more closely coupled, and the simulated amplitude ratio approaches 1 and the simulated phase shift approaches 0.

4. Application to a Field Case

In this section we apply our model to interpret the tidal response of water level in a groundwater well (the Lijiang well) in southwestern China. The well is screened in a thick (143 m) aquifer of mid-Triassic, fine-

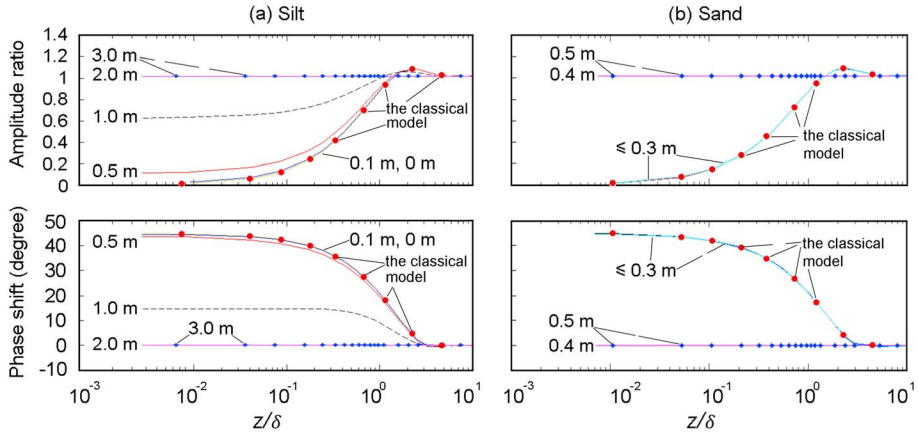

Figure 3. Simulated amplitude ratio and phase shift of the tidal response of pressure head in unconfined aquifers composed of (a) silt and (b) sand, plotted against the normalized depth of the water table z/δ (see text for definition of δ). Numbers marked next to each curve show the average water table depth in the simulation. Red solid circles denote the predicted response for the traditional model of unconfined aquifers.

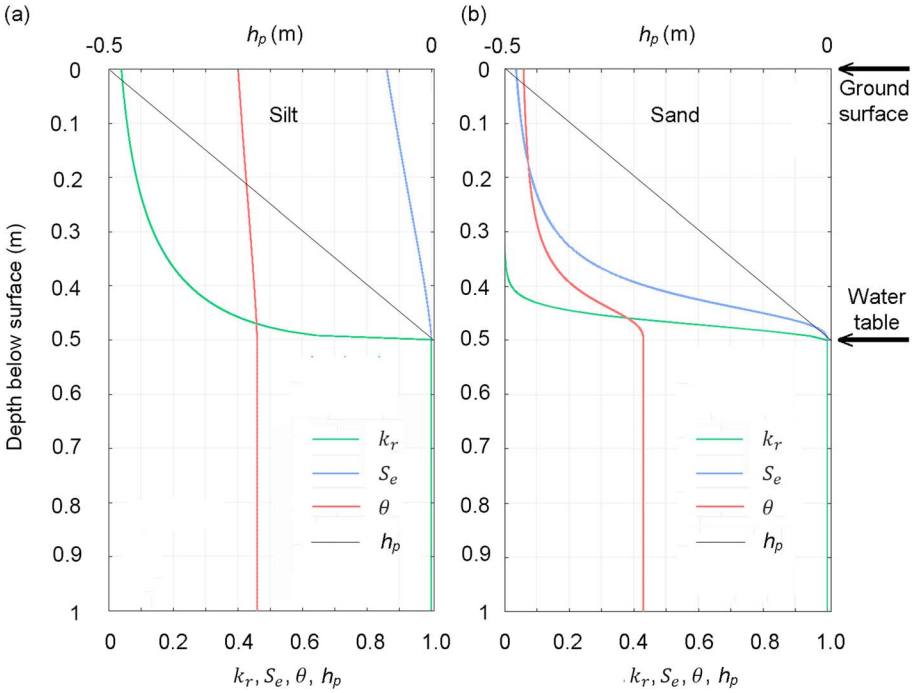

Figure 4. Predicted changes in water content, relative saturation and hydraulic conductivity, and pressure head in (a) a silt aquifer and (b) a sand aquifer above and below the water table. Data used for these predictions are given in Table 1. Notice the sharp changes of these parameters in the sand aquifer and the relatively gentle changes in the silt aquifer. The average depth of the water table is set to 0.5 m.

grained carbonate rocks with a horizontal transmissivity of ~0.1 m^2/s (Liao & Wang, 2018), which corresponds to a horizontal conductivity of 1.3×10^{-3} m/s. Before 2011 the average water level in this well was above ground (Figure 5a); the water level dropped below the ground surface after 2011, likely due to regional over-withdrawal of groundwater. Following 2011, the water table is below the ground surface for most of the year but rises annually to the surface during the rainy season (Figure 5a).

The water level data (Figure 5a) show excellent tidal response (Figure 5b). Water table data before 2011 was not analyzed because nondocumented loss of water occurred when hydraulic heads were above the ground surface, which makes the data not appropriate for this study. Tidal analysis of the data after 2011 shows nearly constant phase at ~0° and amplitude ratio ~1 to the M_2 tide when the water table is more than 2 m below the surface (Figure 6); but when the water table rises above ~2 m below the surface, the phase shift increases from ~0° to ~20° and the amplitude ratio decreases from ~1 to ~0.7. Liao and Wang (2018) interpreted this change in tidal response with the traditional model for unconfined aquifers and proposed that permeability is seasonally enhanced sixfold when the water table rises above ~2 m below the surface. Here we propose an alternative hypothesis that these changes may be due to the rise of the water table to the ground surface that causes an annual transition of the water table from a capillary-affected state to a capillary-free state. In the following paragraph we test the validity of this hypothesis with numerical simulation.

As Liao and Wang (2018) pointed out, the average water level in this well was above ground before 2011 (Figure 5a) but dropped below the ground surface after 2011. Loss of water due to overflow when the water level was above ground was not documented; thus, the present analysis is limited to data after 2011. The aquifer sampled by this well is semiconfined and has high horizontal transmissivity (0.1 m^2/s). Because of the high transmissivity, its tidal response is insensitive to changes in horizontal flow (Doan et al., 2006; Hsieh et al., 1987) and any change of the tidal response must solely be due to changes in vertical flow. We simulate the tidal response with a vertical flow model based on equation (7) not only because it is consistent with the procedure in Liao and Wang (2018), whose interpretation we compare directly, but also because this

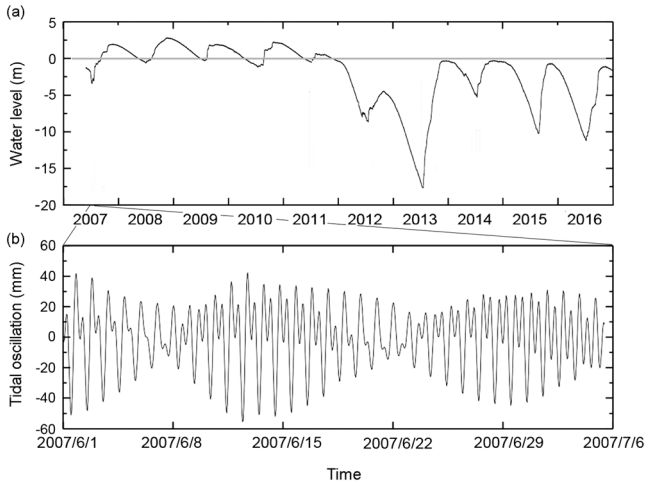

Figure 5. (a) Time series of water level in the Lijiang well, from the beginning of 2007 to the end of 2016. Notice the large fluctuations of water level in this well and that the water level was mostly above ground surface before 2011 but was below the ground surface after 2011. (b) Enlarged portion of the time series showing the tidal oscillations of water level in the Lijiang well (modified from Liao & Wang, 2018).

is the only available model that includes the effect of capillary action in simulating aquifer response to solid tides.

Numerical experiments show that the simulated tidal response is sensitive to the parameters K_s and S_s but less sensitive to the other parameters (supporting information). Since no experimental data exist for the unsaturated fine-grained carbonate rocks of this aquifer, we use parameter sweep and optimization to search for the parameters that best fit the observed tidal response (Table 1). The results of the simulation are plotted as stars in Figure 6 and compared with observations of both the phase and amplitude. The good agreement between the observed and the simulated tidal responses suggests that the change of the tidal response in the Lijiang well with the change in the water table depth may be naturally explained by the transition of the water table from a capillary-affected state, when the water table is below the ground surface, to a capillary-free state, when the water table rises annually to the ground surface during rainy season.

5. Discussion

In this section we discuss several aspects and assumptions of the model and its implications for geologic processes.

5.1. Seasonal Permeability Enhancement?

Liao and Wang (2018) used the traditional model for unconfined aquifer to interpret the tidal response in the Lijiang well and arrived at the conclusion that the permeability of the aquifer may have been seasonally enhanced sixfold when the water table rises to the surface. If correct, the model would have important implications on the basic behaviors of groundwater systems. However, the suggested seasonal change of aquifer permeability has not been demonstrated experimentally or supported theoretically; thus, it remains speculative at this stage. The present interpretation of the same tidal response, on the other hand, is based on sound theoretical formulation and numerical simulation constrained by experimental data and thus has a more rigorous foundation. It suggests instead that the change in the tidal response may be due to a transition of the water table from one affected by the capillary zone to one without a capillary zone when the water table rises to the surface. Thus, it is probably unnecessary to hypothesize a seasonal enhancement of permeability to explain the seasonal change of the tidal response of groundwater in the Lijiang well. The contrast between the two studies illustrates the importance in choosing the correct model for the interpretation of aquifers' tidal response; drastically different interpretations of the subsurface transport processes may be made from the same observation using different models.

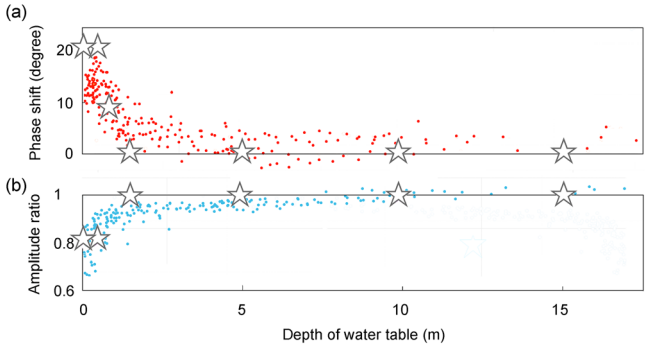

Figure 6. Observed (a) phase shift (red dots) and (b) amplitude ratio (blue dots) of the tidal response to the M_2 tide in the Lijiang well plotted against the water table depth (from Liao & Wang, 2018). Simulated phase shift and amplitude ratio with the hydraulic parameters listed in the last column of Table 1 are plotted as stars. Notice that the phase shift is close to 0 and the amplitude ratio is close to 1 when the water level depth is more than 2 m, but the phase shift increases while the amplitude ratio decreases when the water table becomes shallower than 2 m below the ground surface.

A cautionary note regarding the above interpretation needs to be added here. The hydrogeological settings around the Lijiang well is complex, but the model used in the interpretation is very simple. The aquifer sampled by the Lijiang well is composed of fine-grained carbonate rocks that are heterogeneous and consists of limestone, dolomite, and breccia (e.g., Liao & Wang, 2018). Thus, the use of a single set of hydrological parameters (Table 1) to represent the whole aquifer can only be regarded as a gross approximation. Furthermore, the exposed part of the formation that forms the aquifer sampled by the Lijiang well shows complex paleokarst features such as dissolution cavities, collapse breccias, enlarged fractures by dissolution, and locally extensive vuggy porosity. These features are likely to further complicate the hydrogeology of the well. Thus, the application of the present model to study the tidal response at the well may only be regarded as a first approximation. Additional tests are needed to evaluate the tidal response of the well and the effects of these complications when better models become available.

5.2. Capillary Zone Above a Moving Water Table

In our numerical simulations, the capillary zone above the water table is simulated with the tabulated hydraulic properties of unsaturated sediments (Table 1). Thus, it is implicitly assumed in the simulation that the capillary zone does not change its characteristics with the water table movement. This assumption may be justified in part by the experimental result that shows that the measured hydraulic properties themselves are not functions of time (Table 1) and in part by the fact that the capillary zone is not stagnant but may adjust its position with the moving water table. Laboratory experiments show that the capillary zone above the water table can readily adjust its position as the water table moves (e.g., Nielsen & Perrochet, 2000); thus, if the movement of the water table is slow enough, one may expect that the capillary fringe above the moving water table will adjust accordingly and stay unchanged. Barry et al. (1996) suggested an analytical criterion, based on the approximate solution of a modified Boussinesq equation, that, responding to periodic ocean-wave loading at the coast, the capillary fringe in an unconfined aquifer may significantly affect the water table oscillations unless the ratio $K/(\omega B) \gg 1$, where K is the hydraulic conductivity, B the effective thickness of the capillary fringe, and ω the angular frequency of the water-level oscillation. Applying this criterion to the present study, with $K \sim 10^{-6}$ m/s (Table 1) and $B \sim 1.6$ m (Fetter, 1999) for a silt aquifer, $K/(\omega B) \sim 0.006$ for the angular frequency of the M_2 tide ($\omega \sim 1.4 \times 10^{-4}$ s^{-1}). Thus, the criterion by Barry et al. (1996) would suggest that the capillary fringe in a silt aquifer would have significant effects on the water table response to the M_2 tide, consistent with the present results. For the sand aquifer, on the other hand, with $B \sim 0.17$ m (Fetter, 1999) and $K \sim 10^{-4}$ m/s (Table 1), we have $K/(\omega B) \sim 6$; thus, assuming the same criterion, the capillary effect in a sand aquifer may be marginal in influencing the water table response to Earth tides. More experimental and theoretical studies are needed to verify if the capillary effect in an unconfined sand aquifer may or may not influence the water table response to Earth tides.

5.3. Capillarity and Pore Pressure in Unconfined Aquifers

We argued that the capillary zone may remain unchanged above a slowly moving water table driven by Earth tides. In contrast, the capillary zone may drastically change when it is intercepted by the ground surface. Meyboom (1967) observed that the rise in the water table during precipitation is frequently much greater in magnitude than would be predicted from the amount of precipitation and the specific yield of the aquifer. Gillham (1984) showed that the addition of a small amount of water can lead to an immediate and large rise in the water table if the saturated zone of the capillary zone extends to ground surface. Turner and Nielsen (1997) measured pore pressure beneath ocean beaches in the surf zone and found that pore pressure oscillates at amplitudes much greater than that due directly to the change of surface pressure during the swash; they attributed this fluctuation of pressure to the appearance and disappearance of meniscuses at the sand surface during the swash. The present study complements these studies by showing that the tidal response of unconfined aquifer changes drastically with the presence or absence of the capillary zone. These different observations may share the same physical basis that they are all caused by the destruction of the capillary zone, either by the intersection of the capillary zone with the ground surface, by infiltrated water during precipitation, or by swash in the surf zone.

6. Concluding Remarks

Interpretation of the response of unconfined aquifers to Earth tides in the past 50 years has been based on a traditional model that assumes free drainage of groundwater to the water table. In this study we use numerical simulation that couples poroelastic tidal strain and groundwater flow in the saturated and the unsaturated zones to show that the traditional model correctly predicts the tidal response only when the water table rises to the surface and the capillary zone disappears. But when the water table is below the surface and overlain by a capillary zone, the predicted tidal response of the traditional model departs significantly from the numerical results. Applying the numerical model to a field case where large seasonal changes of tidal response have been documented, we show that the seasonal change in the tidal response may be due to the change of the capillary zone when it is intercepted by the ground surface as the water table rises to the surface. Thus, the interpretation of the tidal response of unconfined aquifers without considering the capillary effect may lead to incorrect inferences of subsurface processes and properties.

Acknowledgments

We thank Lian Xue, Xiaojing Fu, Steve Breen, Zheming Shi, three reviewers, and the Associate Editor for reading the manuscript and providing helpful comments; Chen-Chen Song for helping with the parameter optimization; and Huai Zhang for comments on the numerical computation. Work was partly supported by NSF Grant EAR1344424. Data in this work are from Liao and Wang (2018); no new data are used.

References

Allègre, V., Brodsky, E. E., Xue, L., Nale, S. M., Parker, B. L., & Cherry, J. A. (2016). Using earth-tide induced water pressure changes to measure in situ permeability: A comparison with long-term pumping tests. *Water Resources Research*, *52*, 3113–3126. https://doi.org/10.1002/2015WR017346

Barbour, A. J., Xue, L., Roeloffs, E., & Rubinstein, J. L. (2019). Leakage and increasing fluid-pressure detected in Oklahoma's wastewater disposal reservoir. *Journal of Geophysical Research: Solid Earth*, *124*, 2896–2919. https://doi.org/10.1029/2019JB017327

Barry, D. A., Barry, S. J., & Parlange, J.-Y. (1996). Capillarity correction to periodic solutions of shallow flow approximation. *Coastal and Estuarine Studies*, *50*, 495–510.

Bear, J. (1972). *Dynamics of fluids in porous media*. New York: Dover.

Biot, M. A. (1941). General theory of three-dimensional consolidation. *Journal of Applied Physics*, *12*(2), 155–164. https://doi.org/10.1063/1.1712886

Bower, D. R., & Heaton, K. C. (1978). Response of an aquifer near Ottawa to tidal forcing and the Alaskan earthquake of 1964. *Canadian Journal of Earth Sciences*, *15*(3), 331–340. https://doi.org/10.1139/e78-039

Bredehoeft, J. D. (1967). Response of well-aquifer systems to Earth tides. *Journal of Geophysical Research*, *72*(12), 3075–3087. https://doi.org/10.1029/JZ072i012p03075

Carsel, R. F., & Parrish, R. S. (1988). Developing joint probability distributions of soil water retention characteristics. *Water Resources Research*, *24*(5), 755–769. https://doi.org/10.1029/WR024i005p00755

Cartwright, N., Nielsen, P., & Li, L. (2005). Experimental observations of watertable waves in an unconfined aquifer with a sloping boundary. *Advances in Water Resources*, *27*, 991–1004.

Chui, T.F.M., and D.L. Freyberg (2009), Implementing hydrologic boundary conditions in a multiphysics model, *Journal of Hydrologic Engineering*, *14*, ISSN 1084-0699/2009/12-1374–1377.

Corey, A. T. (1957). Measurement of water and air permeability in unsaturated soils. *Proceedings Soil Science of America*, *21*(1), 7–10. https://doi.org/10.2136/sssaj1957.03615995002100010003x

Doan, M. L., Brodsky, E. E., Prioul, R., & Signier, C. (2006). Tidal analysis of borehole pressure: A tutorial, Schlumberger-Doll Research Report, Cambridge, Mass. Retrieved from https://isterre.fr/IMG/pdf/tidal_tutorial_SDR.pdf

Elkhoury, J. E., Brodsky, E. E., & Agnew, D. C. (2006). Seismic waves increase permeability. *Nature*, *411*, 1135–1138.

Fetter, C. W. (1999). *Contaminant hydrogeology*. Upper Saddle River, NJ: Prentice Hall.

Fetter, C. W. (2001). *Applied hydrogeology*, (4th ed.). Upper Saddle River, NJ: Prentice Hall.

Fredlund, D. G., & Xing, A. Q. (1994). Equations for the soil-water characteristic curve. *Canadian Geotechnical Journal*, *31*(4), 521–532. https://doi.org/10.1139/t94-061

Gillham, R. W. (1984). The capillary fringe and its effect on water-table response. *Journal of Hydrology*, *67*(1-4), 307–324. https://doi.org/10.1016/0022-1694(84)90248-8

Green, D. H., & Wang, H. F. (1990). Specific storage as a poroelastic constant. *Water Resources Research*, *26*(7), 1631–1637. https://doi.org/10.1029/WR026i007p01631

Hsieh, P. A., Bredehoeft, J. D., & Farr, J. M. (1987). Determination of aquifer transmissivity from earth tide analysis. *Water Resources Research*, *23*, 1824–1832.

Kong, J., Shen, C.-J., Xin, P., Song, Z., Li, L., Barry, D. A., et al. (2013). Capillary effect on water table fluctuations in unconfined aquifers. *Water Resources Research*, *49*, 3064–3069. https://doi.org/10.1002/wrcr.20237

Li, L., Barry, D. A., Parlange, J.-Y., & Pattiaratchi, C. B. (1997). Beach water table fluctuations due to wave run-up: Capillarity effects. *Water Resources Research*, *33*(5), 935–945. https://doi.org/10.1029/96WR03946

Liao, X., & Wang, C.-Y. (2018). Seasonal permeability change of the shallow crust inferred from deep well monitoring. *Geophysical Research Letters*, *45*, 11,130–11,136. https://doi.org/10.1029/2018GL080161

Meinzer, O.E. (1923). Outline of ground-water hydrology, with definitions, US Geol Surv., Water Suppl. Paper 494.

Meyboom, P. (1967). Groundwater studies in the Assiniboine River drainage basin, Part II. Hydrologic characteristics of phreatophytic vegetation in south-central Saskatchewan. *Bulletin of the Geological Survey of Canada*, *139*, 18–23.

Mualem, Y. (1976). A new model for predicting the hydraulic conductivity of unsaturated porous media, *Water Resources Research*, *12*, 513–522.

Muñoz, J.J., Lloret, A. & Alonso, E. (2003). Laboratory report: Characterization of hydraulic properties under saturated and non saturated conditions, Project Deliverable D4, VE project (FIKW-CT2001-00126).

Nielsen, P., & Perrochet, P. (2000). Watertable dynamics under capillary fringes: Experiments and modeling. *Advances in Water Resources*, *23*(5), 503–515. https://doi.org/10.1016/S0309-1708(99)00038-X

Parlange, J.-Y., & Brutsaert, W. (1987). A capillarity correction for free surface flow of groundwater. *Water Resources Research*, *23*(5), 805–808. https://doi.org/10.1029/WR023i005p00805

Pliny the Elder (circa AD 77–79) (n.d.). *The natural history, Book II*, Chapter 80 https://archive.org/stream/plinysnaturalhis00plinrich#page/n125/mode/2up.

Richards, L. A. (1931). Capillary conduction of liquids through porous mediums. *Physics*, *1*(5), 318–333. https://doi.org/10.1063/1.1745010

Roeloffs, E. (1996). Poroelastic techniques in the study of earthquake related hydrologic phenomena. *Advances in Geophysics*, *37*, 135–195. https://doi.org/10.1016/S0065-2687(08)60270-8

Rojstaczer, S. (1988). Determination of fluid flow properties from the response of water levels in wells to atmospheric loading. *Water Resources Research*, *24*(11), 1927–1938. https://doi.org/10.1029/WR024i011p01927

Rojstaczer, S., & Riley, F. S. (1990). Response of the water level in a well to Earth tide and atmospheric loading under unconfined conditions. *Water Resources Research*, *26*(8), 1803–1817. https://doi.org/10.1029/WR026i008p01803

Shoushtari, S. M. H. J., Nielsen, P., Cartwright, N., & Perrochet, P. (2015). Periodic seepage face formation and water pressure distribution along a vertical boundary of an aquifer. *Journal of Hydrology*, *523*, 24–33. https://doi.org/10.1016/j.jhydrol.2015.01.027

Turner, I. L., & Nielsen, P. (1997). Rapid water table fluctuations within the beach face: Implications for swash zone sediment mobility? *Coastal Engineering*, *32*(1), 45–59. https://doi.org/10.1016/S0378-3839(97)00015-X

Van Genuchten, M. (1980). A closed-form equation for predicting the hydraulic of conductivity of unsaturated soils. *Soil Science Society of America Journal*, *44*(5), 892–898. https://doi.org/10.2136/sssaj1980.03615995004400050002x

Villar, M.V. (2007). Retention curves determined on samples taken before the second drying phase. Technical report M2144/5/07. Madrid: CIEMAT.

Wang, C.-Y., Doan, M.-L., Xue, L., & Barbour, A. J. (2018). Tidal response of groundwater in a leaky aquifer—Application to Oklahoma. *Water Resources Research*, *54*, 8019–8033. https://doi.org/10.1029/2018WR022793

Wang, H. F. (2000). *Theory of linear poroelasticity*, *Princeton Ser. Geophys.* Princeton, NJ: Princeton University Press.

Xue, L., Brodsky, E. E., Erskine, J., Fulton, P. M., & Carter, R. (2016). A permeability and compliance contrast measured hydrogeologically on the San Andreas Fault. *Geochemistry, Geophysics, Geosystems*, *17*, 858–871. https://doi.org/10.1002/2015GC006167